ACS APPLIED MATERIALS & INTERFACES

Research Article

www.acsami.org

Improvement in Negative Bias Stress Stability of Solution-Processed Amorphous In−Ga−Zn−O Thin-Film Transistors Using Hydrogen Peroxide

Jeong Moo Kwon, Joohye Jung, You Seung Rim, Dong Lim Kim, and Hyun Jae Kim*

School of Electrical and Electronic Engineering, Yonsei University, 50 Yonsei-ro, Seodaemun-gu, Seoul 120-749, Korea

ABSTRACT: We have investigated the effect of hydrogen peroxide (H_2O_2) on negative bias stress (NBS) stability of solution-processed amorphous indium−gallium−zinc oxide (a-IGZO) thin-film transistors (TFTs). The instability of solution-processed a-IGZO TFTs under NBS is attributed to intrinsic oxygen vacancy defects (V_o) and organic chemical-induced defects, such as pores, pin holes, and organic residues. In this respect, we added H_2O_2 into an indium−gallium−zinc oxide solution to reduce the defects without any degradation of electrical performance. The field-effect mobility and sub-threshold slope of the a-IGZO TFTs were improved from 0.37 $cm^2 V^{-1} s^{-1}$ and 0.86 V/dec to 0.97 $cm^2 V^{-1} s^{-1}$ and 0.58 V/dec, respectively. Furthermore, the threshold voltage shift under NBS was dramatically decreased from −3.73 to −0.18 V. These results suggest that H_2O_2 effectively reduces V_o through strong oxidation and minimizes organic chemical-induced defects by eliminating the organic chemicals at lower temperatures compared to a conventional solution process.

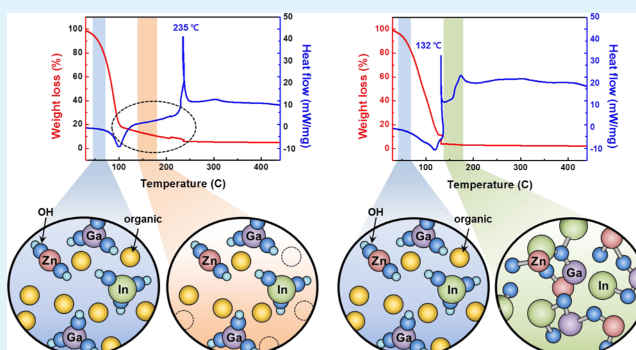

KEYWORDS: *oxide semiconductor, thin-film transistors, solution process, hydrogen peroxide, indium−gallium−zinc oxide*

1. INTRODUCTION

Amorphous metal oxide semiconductors (AOS) have attracted considerable attention as promising alternatives to conventional hydrogenated amorphous silicon (a-Si:H) and poly-crystalline silicon (poly-Si) for use as the backplane in active-matrix displays. AOS thin-film transistors (TFTs) have better electrical characteristics than a-Si:H TFTs, exhibiting high carrier mobility because of the high symmetry of s orbitals in heavy metal ions and high transparency derived from a relatively large band gap.[1−4] Additionally, AOS TFTs provide better electrical uniformity than laser-crystallized poly-Si TFTs. To date, research about AOS TFTs has focused on three main areas: the role of individual metal elements in multi-component oxide semiconductor systems,[5−8] thin-film formation with high performance and low temperature for flexible devices,[9−14,38−40] and stability against bias, temperature, and the presence of ambient gases.[15−22] Most of these studies have involved vacuum-processed AOS TFTs. Previous reports regarding the instability of AOS TFTs have suggested that the mechanism responsible for the threshold voltage shift (ΔV_{th}) under negative bias stress (NBS) is related to the charge trapping of photo-generated hole by light illumination occurring at the interface between the channel and gate insulator (G/I) or injection into the G/I bulk.[15−18,23−25] This mechanism seems plausible for vacuum-processed devices. In vacuum-processed AOS TFTs, under NBS and without light illumination, ΔV_{th} is negligible and no significant degradation occurs in electrical performance, such as field-effect mobility (μ_{FE}) and sub-threshold slope (S·S). However, solution-processed AOS TFTs exhibit poor stability under NBS in the absence of light illumination, and electrical performance is degraded to some extent. This suggests that solution-processed AOS TFTs have another mechanism that causes instability under NBS besides photo-generated hole. This is likely related to the organic chemicals that are used in the solution process but not in the vacuum process. The organic chemicals used in the solution process cause structural defects, such as pores or pin holes, through volatilization during the annealing process.[26] Moreover, organic residues can easily be captured by these structural defects and act as impurities after they are trapped in the thin-film bulk. Therefore, solution-processed AOS TFTs are less stable than vacuum-processed AOS TFTs and, therefore, are not yet commercialized, although the solution process is a promising method because it offers competitive features, such as low cost, simplicity, and high throughput. Nowadays, vacuum-processed AOS TFTs are only in use in the display industry.

Solution-processed AOS TFTs have two typical defects: intrinsic oxygen vacancy defects (V_o) and organic chemical-induced defects. Researchers have developed several methods to reduce V_o using additional processing, such as high-pressure oxygen annealing and ozone-plasma treatment,[15,16] and some

Received: November 27, 2013
Accepted: February 6, 2014
Published: February 6, 2014

 © 2014 American Chemical Society

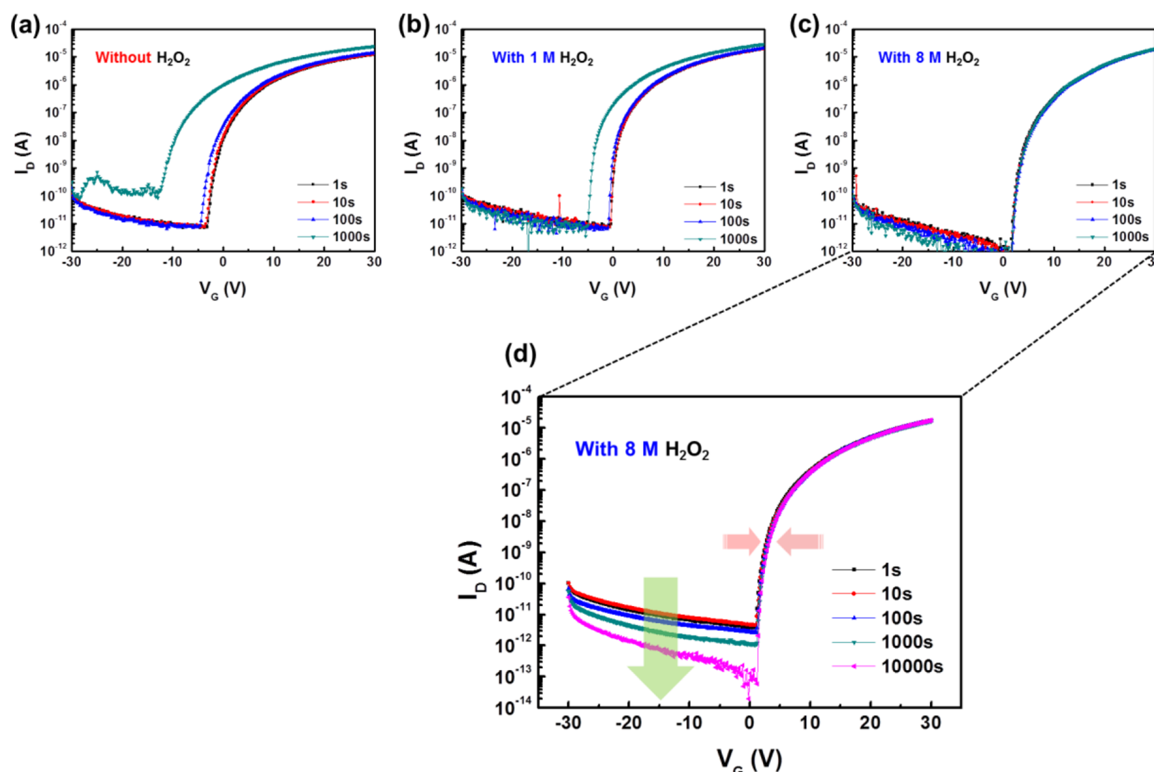

Figure 1. Evolution of transfer curves as a function of stress time under NBS for a-IGZO TFTs with differing amounts of H_2O_2 in dark conditions: (a) without H_2O_2, (b) with 1 M H_2O_2, and (c) with 8 M H_2O_2. (d) Result of re-testing of sample c for reproducibility 3 months later (with stress time extended to 10^4 s).

papers have been reported to remove the organic chemicals by ultraviolet irradiation.[13,14,27] However, these methods require additional processes and expensive equipment, such as vacuum, high-pressure, and ultraviolet facilities.

In this paper, we suggest a new and simple approach to improve stability in solution-processed AOS TFTs under NBS, focusing on the amorphous indium−gallium−zinc oxide (a-IGZO) TFTs. Employing hydrogen peroxide (H_2O_2) in the solution process helps reduce defects at the interface between channel and G/I through strong oxidation and minimizes organic chemical-induced defects, such as pores, pin holes, and organic residues, through decomposing organic chemicals at low temperatures. The results indicate that employing H_2O_2 in a solution process is an effective method to improve stability under NBS and can likely be applied to various solution-processed AOS TFTs besides a-IGZO TFTs.

2. EXPERIMENTAL PROCEDURE

The solution for a-IGZO TFTs was prepared by dissolving indium nitrate hydrate [$In(NO_3)_3 \cdot xH_2O$], gallium nitrate hydrate [$Ga(NO_3)_3 \cdot xH_2O$], and zinc acetate dihydrate [$Zn(CH_3COO)_2 \cdot 2H_2O$] as precursors into a 2-methoxyethanol ($CH_3OCH_2CH_2OH$) solvent. The total molarity of indium−gallium−zinc oxide (IGZO) solution was 0.3 M with a In/Ga/Zn mole ratio of 5:1:2. The 1.0 M monoethanolamine (MEA) and 1.5 M acetic acid (CH_3COOH) were added to stabilize the solution, to control pH, and to enhance homogeneity of the solution. To compare the effect of adding H_2O_2 into the solution, we synthesized three types of solutions: one without H_2O_2, one with 1 M H_2O_2, and another with 8 M H_2O_2.

To fabricate bottom-gate-structured TFTs, the prepared solutions were spin-coated at 3000 rpm for 30 s onto heavily doped p-type Si wafers, upon which a 1200 Å thick layer of SiO_2 as G/I was grown through thermal oxidation. The coated films were baked for 30 min at 100 °C to activate H_2O_2. All samples, including the one without H_2O_2, underwent the same activation process to rule out the effect of annealing time. Subsequently, the samples were pre-baked for 5 min at 300 °C and then post-annealed for 2 h at 400 °C. After forming the active layer, source and drain electrodes with a 200 nm thick layer of Al were deposited via radio frequency (rf) magnetron sputtering with a shadow mask. Finally, we obtained three types of a-IGZO TFTs with 1000 μm channel width and 150 μm channel length without passivation.

The current−voltage ($I-V$) characteristics of the a-IGZO TFTs were extracted using an Agilent HP4156C semiconductor analyzer in the dark and an atmospheric condition. We also carried out thermogravimetry and differential scanning calorimetry (TG−DSC) to clarify the effect of H_2O_2 as a decomposer of the organic chemicals.

3. RESULTS AND DISCUSSION

Figure 1 shows the evolution of transfer curves of a-IGZO TFTs with different amounts of H_2O_2 as a function of stress time under NBS in the absence of light. The devices were stressed under conditions where the gate voltage (V_G), drain voltage (V_D), and time duration were set at −20 V, 10.1 V, and 10^3 s at room temperature, respectively. In Figure 1a, the transfer curve of a-IGZO TFT without H_2O_2 shifted considerably in the negative direction with increasing NBS time. In contrast, the transfer curve of a-IGZO TFT with 1 M H_2O_2 in Figure 1b shifted less in the negative direction, and the transfer curve of a-IGZO TFT with 8 M H_2O_2 hardly shifted, as shown in Figure 1c. Furthermore, we measured sample c again 3 months later with an extended stress time from 1 to 10^4 s to verify reproducibility; the result indicated that the transfer curve was rigid like the preceding result for sample c, as shown in Figure 1d. The off state in Figure 1d was different compared to Figure 1c, which is attributed to the effect of the exposed surface of a-IGZO TFTs without passivation.[21,22,36,37] How-

ever, the remarkable point is that there was little shift of transfer curves under NBS in Figure 1d, which indicated that the effect of addition of H_2O_2 lasted for a reasonable period of time. As a result, increasing amounts of H_2O_2 decreased the negative shift in transfer curves of a-IGZO TFTs under NBS and improved stability. Figure 2 shows that the variation in ΔV_{th} of a-IGZO TFTs under NBS decreased with increasing amounts of H_2O_2, in accordance with the results seen in Figure 1. The ΔV_{th} under NBS is attributed to hole trapping at the interface between the channel and G/I or hole injection into the G/I bulk.[18,25,28,29] Previous research has suggested that hole-trapping sites of a-IGZO TFTs under NBS originate from V_o,[25] but the origin of hole-trapping sites is still controversial. Our findings suggest that organic chemical-induced defects in solution-processed a-IGZO TFTs can act as hole-trapping sites, suggesting that organic chemical-induced defects influence the stability under NBS.

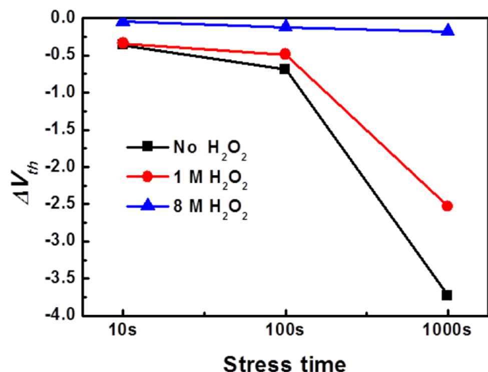

Figure 2. Variation of the threshold voltage shift (ΔV_{th}) as a function of stress time under NBS for a-IGZO TFTs with differing amounts of H_2O_2.

Table 1 summarizes the electrical parameters of a-IGZO TFTs without H_2O_2, with 1 M H_2O_2, and with 8 M H_2O_2.

Table 1. Electrical Characteristics of a-IGZO TFTs without H_2O_2, with 1 M H_2O_2, and with 8 M H_2O_2

	mobility ($cm^2 V^{-1} s^{-1}$)	on/off current ratio	S·S (V/dec)	N_t (#/cm^2)
no H_2O_2	0.37	1.71×10^6	0.86	2.3×10^{12}
1 M H_2O_2	0.67	2.77×10^6	0.61	1.7×10^{12}
8 M H_2O_2	0.97	5.17×10^7	0.58	1.5×10^{12}

Noticeable differences were observed in μ_{FE}, on/off current ratio (I_{on}/I_{off}), S·S, and interface trap density (N_t). The μ_{FE} and I_{on}/I_{off} values increased and S·S and N_t values decreased with increasing amounts of H_2O_2. These results indicate that the defects in a-IGZO TFTs decrease with increasing amounts of H_2O_2 and, thereby, improve electrical performance and stability.

The addition of H_2O_2 into IGZO solution can affect three aspects: interface, bulk, and surface of a-IGZO TFTs. Figure 3 shows the effect of H_2O_2 on three aspects of a-IGZO TFTs by comparing the stability of a-IGZO TFTs under NBS with double top/bottom structures made up of [IGZO/IGZO], [IGZO with H_2O_2/IGZO], [IGZO/IGZO with H_2O_2], and [IGZO with H_2O_2/IGZO with H_2O_2]. Here, the 0.3 M IGZO solution without H_2O_2 and the 0.3 M IGZO solution with 8 M H_2O_2 were chosen as materials of each layer. All a-IGZO TFTs underwent the same annealing process to avoid the effect of annealing time: the bottom layer was annealed for 30 min at 100 °C and subsequently for 1 h at 400 °C, and the top layer was annealed in the same fashion. The negative shift in transfer curves for [IGZO/IGZO with H_2O_2] TFT in Figure 3c was smaller than that for [IGZO with H_2O_2/IGZO] TFT in Figure 3b. Moreover, the negative shift in transfer curves for [IGZO with H_2O_2/IGZO with H_2O_2] TFT in Figure 3d was much smaller than those for [IGZO with H_2O_2/IGZO] TFT in Figure 3b and [IGZO/IGZO with H_2O_2] TFT in Figure 3c. These findings suggest that the reduction in defects at the interface between the IGZO layer and G/I (SiO_2) layer is most dominant and the reduction in defects at the IGZO bulk is more than that of the surface on the IGZO top layer. This indicates that the improved stability under NBS is due to reduction in hole-trapping sites at the interface using H_2O_2. Interestingly, [IGZO/IGZO] TFT was more stable than [IGZO with H_2O_2/IGZO] TFT. This result is attributed to the multi-stacked effect on a-IGZO TFTs with double top/bottom structures. Structural defects, such as pores or pin holes, that occurred in the bottom layer are reduced with filling by the solution during the formation of the top layer.[26] In contrast, pores or pin holes in the bottom layer of [IGZO with H_2O_2/IGZO] TFT do not have enough time to be filled with solution of the top layer, because the H_2O_2-added solution in the top layer oxidized and condensed very quickly through strong oxidation.

A comparison of panels b and c of Figure 3 clearly reveals that H_2O_2 has a greater effect on reducing interface trap defects than reducing the back surface defects by ambient gases under

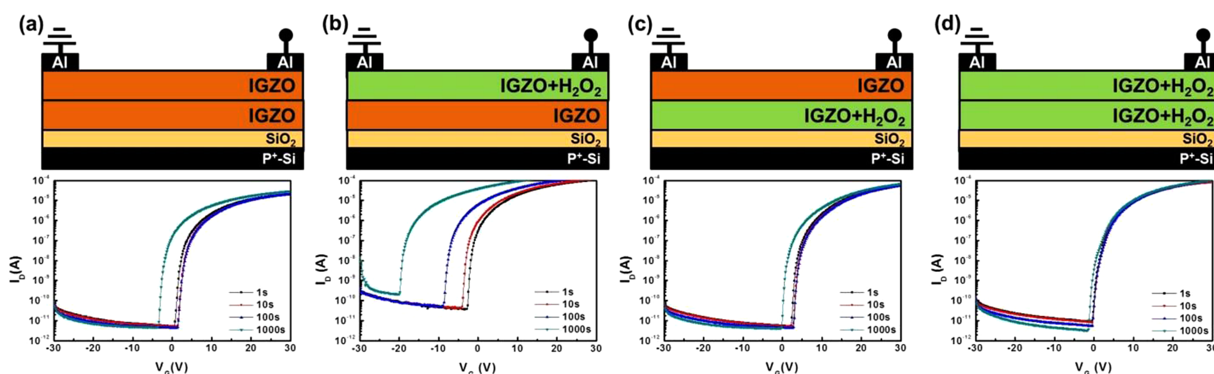

Figure 3. Evolution of transfer curves as a function of stress time under NBS for double-layered a-IGZO TFTs with top/bottom structure: (a) IGZO/IGZO, (b) IGZO (with H_2O_2)/IGZO, (c) IGZO/IGZO (with H_2O_2), and (d) IGZO (with H_2O_2)/IGZO (with H_2O_2).

dx.doi.org/10.1021/am4054139 | ACS Appl. Mater. Interfaces 2014, 6, 3371−3377

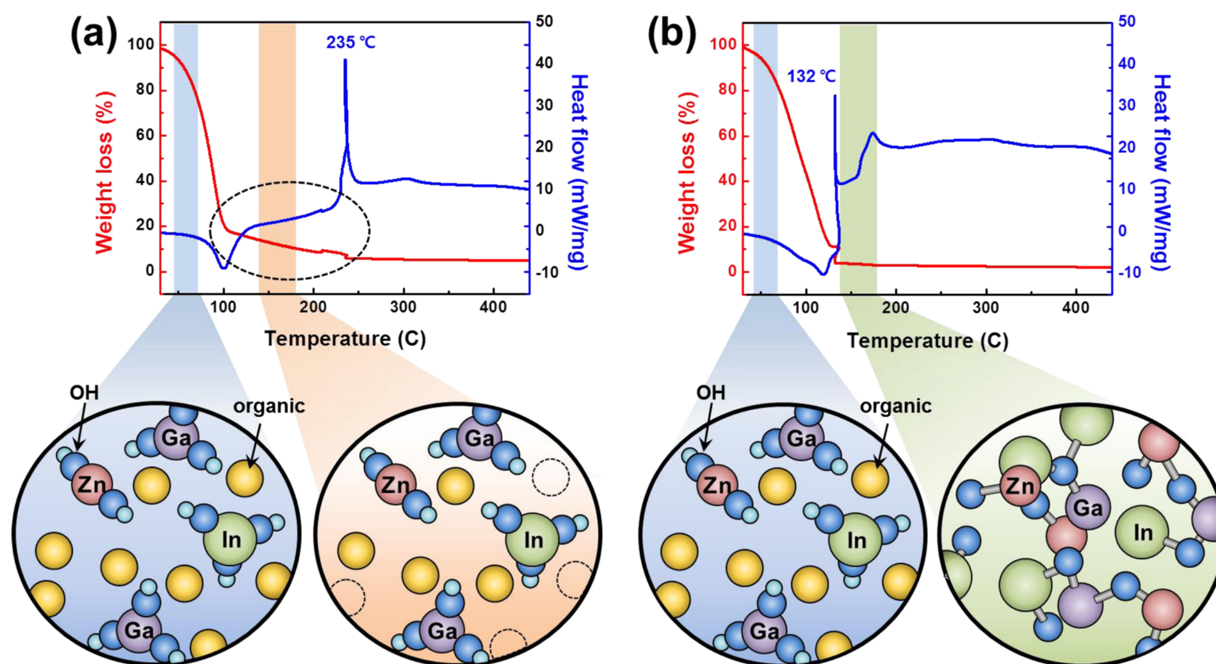

Figure 4. TG−DSC analysis of IGZO solutions (a) without H_2O_2 and (b) with H_2O_2. Circles indicate the different solution states of metal precursors surrounded by organic chemicals in each color-banded region within a temperature range of 0−250 °C.

NBS. The presence of H_2O_2 reduces interface trap defects that act as hole-trapping sites, such as V_o and organic chemical-induced defects, through strong oxidation, thereby improving the stability of a-IGZO TFTs under NBS.

As noted in the Introduction, in solution-processed a-IGZO TFTs, V_o cannot be the only factor affecting stability in a-IGZO TFTs. In contrast to vacuum-processed a-IGZO TFTs, solution-processed a-IGZO TFTs, which require organic chemicals, have other factors that cause instability under NBS, such as unavoidable structural defects (pores and pin holes) and organic residues that act as impurities, because of the volatilization of organic chemicals during the annealing process, and they act as additional hole-trapping sites. Organic chemical-induced defects occur at approximately 150−250 °C during the annealing process. The volatilization of organics consisting of high molecules, such as pure solvent or organic additives, physically damages the structure of the film during gelation and creates pores or pin holes, increasing the likelihood of organic residues in the film. These can act as hole-trapping sites or impurities, which cause instability in a-IGZO TFTs even under dark NBS conditions.

In this study, we found that adding H_2O_2 to the IGZO solution achieved the reduction of organic chemical-induced defects. This finding was verified through TG−DSC analysis of the IGZO solutions with and without the presence of H_2O_2, as shown in Figure 4. In general, the solution process proceeds in three stages.[30] The first stage is defined as a considerable weight loss in solution accompanied by an endothermic reaction, as shown in Figure 4 (red line). During this stage, most of the organic chemicals are vaporized, precursors in the solution are decomposed, and subsequently, hydrolyzed metals are formed, as depicted by M−OH (M, metal; O, oxygen; and H, hydrogen). The second stage begins with film formation, when a large exothermic reaction peak occurs. This exothermic peak signifies the starting point of a film formation, converting M−OH to M−O−M−O (metal−oxygen-network bonding). The third stage denotes a densification process following the exothermic reaction peak. TG−DSC analysis revealed that a significant difference between IGZO solutions with and without H_2O_2 was observed: the exothermic reaction peak in solution without H_2O_2 occurred at 235 °C, as shown in Figure 4a, whereas the exothermic reaction peak in solution with H_2O_2 occurred at 132 °C, as shown in Figure 4b. Moreover, the weight loss curve shown in Figure 4a decreased gradually in the range of 100−235 °C, suggesting that some organic residues remain until 235 °C.[30,31] However, the weight loss curve in Figure 4b decreased abruptly at 132 °C, which indicated that the decomposition of organic residues was accelerated: huge molecules broke down into tiny volatile molecules, such as oxygen, water, and carbon dioxide, through a strong oxidizing reaction of H_2O_2,[32] which were all instantaneously evaporated.

During this process, H_2O_2 is decomposed by pyrolysis and releases hydroxyl radicals ($OH^{\bullet}$) through stepwise reactions below.

$$H_2O_2 \rightarrow 2OH \quad (1)$$

$$OH + H_2O_2 \rightarrow HO_2 + H_2O \quad (2)$$

$$OH + HO_2 \rightarrow H_2O + O_2 \quad (3)$$

The overall reaction by stoichiometric relationship is below.

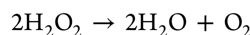

$$2H_2O_2 \rightarrow 2H_2O + O_2$$

All reaction equations are based on related papers.[33,34] Although hydroxyl radicals live a very short time during reactions, they act as a powerful oxidizer. Then, they accelerate the decomposition of organic residues because of a higher oxidation potential than H_2O_2 based on a related paper.[32] The circles in Figure 4 depict the hydrolyzed metals surrounded by organic residues in IGZO solutions at various temperature ranges. In contrast to Figure 4a, the hydrolyzed metals in solution with H_2O_2 in Figure 4b develop metal−oxygen-network bonding at a lower temperature of about 100 °C, which minimizes the possibility of generating defects, such as pores or pin holes, during gelation. It is reasonable to assume

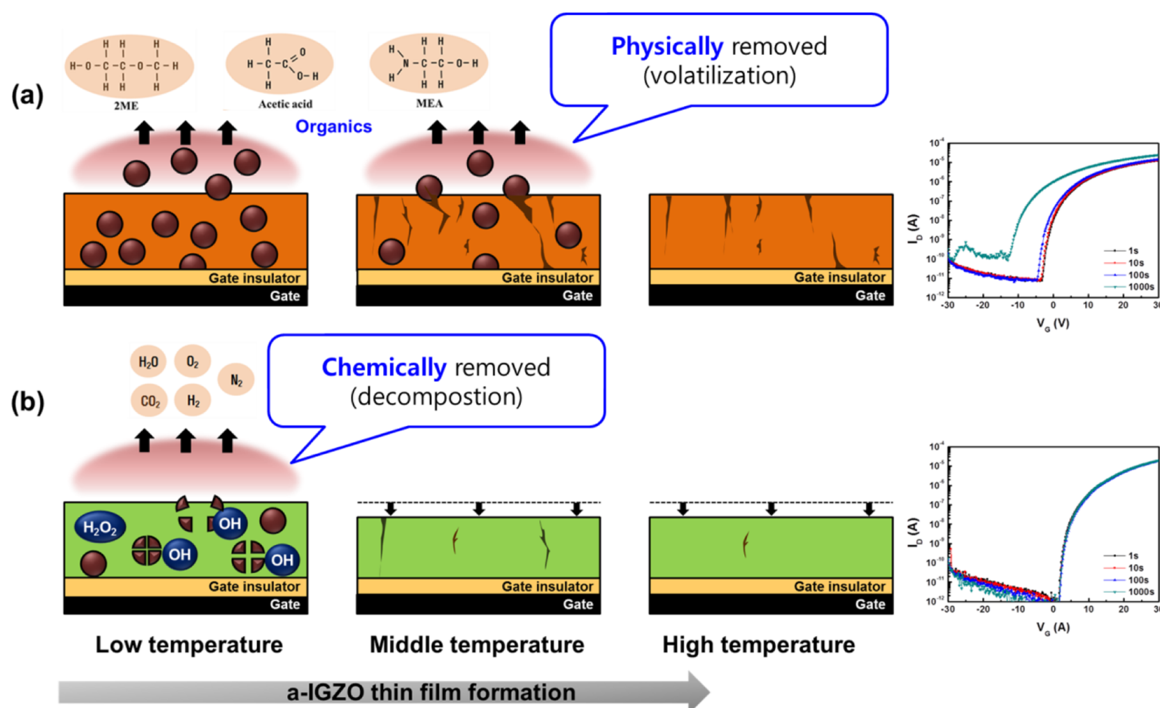

Figure 5. Schematics of the process of generating organic chemical-induced defects, comparing thin-film formation of IGZO solutions (a) without H_2O_2 and (b) with H_2O_2, with an increasing temperature.

that eliminating organic residues chemically at lower temperatures by adding H_2O_2 to the solution diminishes organic chemical-induced defects, such as pores, pin holes, and impurities.

Moreover, adding H_2O_2 to the solution accelerates densification through the chemical removal of organic residues surrounding hydrolyzed metals at lower temperatures compared to a conventional solution process involving physical removal through volatilization.[13,35] Consequently, employing H_2O_2 in a solution process can improve stability under NBS via chemical removal of organic chemical-induced defects at lower temperatures and also accelerates the densification of a-IGZO thin films.[12,13,27]

Figure 5 compares the procedures for removing organic chemicals between IGZO solutions, with and without H_2O_2, during thin-film formation, as the annealing temperature increases. Figure 5a shows that, in solution without H_2O_2, organic chemicals remain until a middle temperature of approximately 235 °C and generate organic chemical-induced defects via physical volatilization of organic residues during gelation. Figure 5b shows that, in solutions with H_2O_2, organic chemicals are decomposed chemically at much lower temperatures (132 °C) and removed instantly, which results in minimization of organic chemical-induced defects.

4. CONCLUSION

In this study, we investigated the effects of adding H_2O_2 to a solution process with the goal of improving electrical performance and stability compared to a conventional solution process, with a particular focus on the stability of a-IGZO TFTs under NBS. The solution process is generally accompanied by two typical types of defects as hole-trapping sites: intrinsic V_o and unavoidable organic chemical-induced defects, which are responsible for the instability of a-IGZO TFTs under NBS. We found that H_2O_2 is the efficient additive that reduces those defects simply without requiring any expensive equipment or additional process in the solution process: by reducing V_o at the interface and bulk of a-IGZO TFTs though strong oxidation and also minimizing organic chemical-induced defects through decomposing organic residues chemically from huge molecules to volatile tiny molecules at a much lower temperature (132 °C) than that of pristine a-IGZO TFTs (235 °C). In conclusion, adding H_2O_2 in IGZO solution can improve stability of a-IGZO TFTs under NBS by eliminating the defects that act as hole-trapping sites. This effective treatment is likely also applicable to other oxide TFTs based on the significant improvement in the stability under NBS in a-IGZO TFTs.

AUTHOR INFORMATION

Corresponding Author

*E-mail: hjk3@yonsei.ac.kr.

Notes

The authors declare no competing financial interest.

ACKNOWLEDGMENTS

This work was supported by the Industrial Strategic Technology Development Program (10041808, Synthesis of Oxide Semiconductor and Insulator Ink Materials and Process Development for Printed Backplane of Flexible Displays Processed below 150 °C) funded by the Ministry of Knowledge Economy (MKE, Korea)

REFERENCES

(1) Park, J. S.; Maeng, W.-J.; Kim, H.-S.; Park, J.-S. Review of recent developments in amorphous oxide semiconductor thin-film transistor devices. *Thin Solid Films* **2012**, *520*, 1679−1693.

(2) Hosono, H. Recent progress in transparent oxide semiconductors: Materials and device application. *Thin Solid Films* **2007**, *515*, 6000−6014.

(3) Kamiya, T.; Nomura, K.; Hosono, H. Present status of amorphous In−Ga−Zn−O thin-film transistors. *Sci. Technol. Adv. Mater.* **2010**, *11*, 044305.
(4) Fortunato, E.; Barquinha, P.; Martins, R. Oxide semiconductor thin-film transistors: A review of recent advances. *Adv. Mater.* **2012**, *24*, 2945−2949.
(5) Kim, Y. H.; Han, J. I.; Park, S. K. Effect of zinc/tin composition ratio on the operational stability of solution-processed zinc−tin−oxide thin-film transistors. *IEEE Electron Device Lett.* **2012**, *33* (1), 50−52.
(6) Jeong, S.; Ha, Y. G.; Moon, J.; Facchetti, A.; Marks, T. J. Role of gallium doping in dramatically lowering amorphous-oxide processing temperatures for solution-derived indium zinc oxide thin-film transistors. *Adv. Mater.* **2010**, *22*, 1346−1350.
(7) Rim, Y. S.; Kim, D. L.; Jeong, W. H.; Kim, H. J. Effect of Zr addition on ZnSnO thin-film transistors using a solution process. *Appl. Phys. Lett.* **2010**, *97*, 233502.
(8) Kim, G. H.; Ahn, B. D.; Shin, H. S.; Jeong, W. H.; Kim, H. J. Effect of indium composition ratio on solution-processed nanocrystalline InGaZnO thin film transistors. *Appl. Phys. Lett.* **2009**, *94*, 233501.
(9) Nomura, K.; Takagi, A.; Kamiya, T.; Ohta, H.; Hirano, M.; Hosono, H. Amorphous oxide semiconductors for high-performance flexible thin-film transistors. *Jpn. J. Appl. Phys.* **2006**, *45* (5B), 4303−4308.
(10) Banger, K. K.; Yamashita, Y.; Mori, K.; Peterson, R. L.; Leedham, T.; Rickard, J.; Sirringhaus, H. Low-temperature, high-performance solution-processed metal oxide thin-film transistors formed by a 'sol−gel on chip' process. *Nat. Mater.* **2011**, *10*, 45−50.
(11) Jeong, W. H.; Bae, J. H.; Kim, H. J. High-performance oxide thin-film transistors using a volatile nitrate precursor for low-temperature solution process. *IEEE Electron Device Lett.* **2012**, *33* (1), 68−70.
(12) Kim, M. G.; Kanatzidis, M. G.; Facchetti, A.; Marks, T. J. Low-temperature fabrication of high-performance metal oxide thin-film electronics via combustion processing. *Nat. Mater.* **2011**, *10*, 382−388.
(13) Kim, Y. H.; Heo, J. S.; Kim, T. H.; Park, S.; Yoon, M. H.; Kim, J.; Oh, M. S.; Yi, G. R.; Noh, Y. Y.; Park, S. K. Flexible metal-oxide devices made by room room-temperature photochemical activation of sol−gel films. *Nature* **2012**, *489*, 128−132.
(14) Rim, Y. S.; Jeong, W. H.; Kim, D. L.; Lim, H. S.; Kim, K. M.; Kim, H. J. Simultaneous modification of pyrolysis and densification for low-temperature solution-processed flexible oxide thin-film transistors. *J. Mater. Chem.* **2012**, *22*, 12491.
(15) Ji, K. H.; Kim, J. I.; Jung, H. Y.; Park, S. Y.; Choi, R.; Kim, U. K.; Hwang, C. S.; Lee, D.; Hwang, H.; Jeong, J. K. Effect of high-pressure oxygen annealing on negative bias illumination stress-induced instability of InGaZnO thin film transistors. *Appl. Phys. Lett.* **2011**, *98*, 103509.
(16) Yang, S.; Ji, K. H.; Kim, U. K.; Hwang, C. S.; Park, S. K.; Hwang, C. S.; Jang, J.; Jeong, J. K. Suppression in the negative bias illumination instability of Zn−Sn−O transistor using oxygen plasma treatment. *Appl. Phys. Lett.* **2011**, *99*, 102103.
(17) Yang, B. S.; Park, S.; Oh, S.; Kim, Y. J.; Jeong, J. K.; Hwang, C. S.; Kim, H. J. Improvement of the photo-bias stability of the Zn−Sn−O field effect transistors by an ozone treatment. *J. Mater. Chem.* **2012**, *22*, 10994.
(18) Ji, K. H.; Kim, J.-I.; Mo, Y.-G.; Jeong, J. H.; Yang, S.; Hwang, C.-S.; Park, S.-H. K.; Ryu, M.-K.; Lee, S.-Y.; Jeong, J. K. Comparative study on light-induced bias stress instability of IGZO transistors with SiN_x and SiO_2 gate dielectrics. *IEEE Electron Device Lett.* **2010**, *31* (12), 1404−1406.
(19) Cho, S. H.; Lee, Y. U.; Lee, J. S.; Jo, K. M.; Kim, B. S.; Kong, H. S.; Kwon, J. Y.; Han, M. K. Effect of self-assembled monolayer (SAM) on the oxide semiconductor thin film transistor. *J. Disp. Technol.* **2012**, *8* (1), 35−40.
(20) Huang, S.-Y.; Chang, T.-C.; Chen, M.-C.; Chen, T.-C.; Jian, F.-Y.; Chen, Y.-C.; Huang, H.-C.; Gan, D.-S. Improvement in the bias stability of amorphous InGaZnO TFTs using an Al_2O_3 passivation layer. *Surf. Coat. Technol.* **2013**, *231*, 117−121.
(21) Chen, Y. C.; Chang, T. C.; Li, H. W.; Chen, S. C.; Chung, W. F.; Chen, Y. H.; Tai, Y. H.; Tseng, T. Y.; Yeh(Huang), F. S. Surface states related the bias stability of amorphous In−Ga−Zn−O thin film transistors under different ambient gasses. *Thin Solid Films* **2011**, *520*, 1432−1436.
(22) Liu, P. T.; Chou, Y. T.; Teng, L. F. Environment-dependent metastability of passivation-free indium zinc oxide thin film transistor after gate bias stress. *Appl. Phys. Lett.* **2009**, *95*, 233504.
(23) Oh, H.; Yoon, S.-M.; Ryu, M. K.; Hwang, C.-S.; Yang, S.; Park, S.-H. K. Transition of dominant instability mechanism depending on negative gate bias under illumination in amorphous In−Ga−Zn−O thin film transistor. *Appl. Phys. Lett.* **2011**, *98*, 033504.
(24) Lee, K.-H.; Jung, J. S.; Son, K. S.; Park, J. S.; Kim, T. S.; Choi, R.; Jeong, J. K.; Kwon, J.-Y.; Koo, B.; Lee, S. The effect of moisture on the photon-enhanced negative bias thermal instability in Ga−In−Zn−O thin film transistors. *Appl. Phys. Lett.* **2009**, *95*, 232106.
(25) Ryu, B.; Noh, H. K.; Choi, E. A.; Chang, K. J. O-vacancy as the origin of negative bias illumination stress instability in amorphous In−Ga−Zn−O thin film transistors. *Appl. Phys. Lett.* **2010**, *97*, 022108.
(26) Kim, D. J.; Kim, D. L.; Rim, Y. S.; Kim, C. H.; Jeong, W. H.; Lim, H. S.; Kim, H. J. Improved electrical performance of an oxide thin-film transistor having multistacked active layers using a solution process. *ACS Appl. Mater. Interfaces* **2012**, *4*, 4001−4005.
(27) Weber, D.; Botnaras, S.; Pham, D. V.; Steiger, J.; Cola, L. D. Functionalized ZnO nanoparticles for thin-film transistors: Support of ligand removal by non-thermal methods. *J. Mater. Chem. C* **2013**, *1*, 3098−3103.
(28) Chen, T. C.; Chang, T. C.; Hsieh, T. Y.; Lu, W. S.; Jian, F. Y.; Tsai, C. T.; Huang, S. Y.; Lin, C. S. Investigating the degradation behavior caused by charge trapping effect under DC and AC gate-bias stress for InGaZnO thin film transistor. *Appl. Phys. Lett.* **2011**, *99*, 022104.
(29) Ji, K. H.; Kim, J. I.; Jung, H. Y.; Park, S. Y.; Choi, R.; Mo, Y. G.; Jeong, J. K. Comprehensive studies of the degradation mechanism in amorphous InGaZnO transistors by the negative bias illumination stress. *Microelectron. Eng.* **2011**, *88*, 1412−1416.
(30) Kim, G. H.; Shin, H. S.; Ahn, B. D.; Kim, K. H.; Park, W. J.; Kim, H. J. Formation mechanism of solution-processed nanocrystalline InGaZnO thin film as active channel layer in thin-film transistor. *J. Electrochem. Soc.* **2009**, *156* (1), H7−H9.
(31) Winer, I.; Shter, G. E.; Mann-Lahav, M.; Grader, G. S. Effect of solvents and stabilizers on sol−gel deposition of Ga-doped zinc oxide TCO films. *Mater. Res.* **2011**, *26* (10), 1309−1315.
(32) Izyumov, S. V.; Shchekotov, E. Y.; Shchekotov, D. E.; Tyapkov, V. F.; Erpyleva, S. F.; Bykova, V. V.; Zaitsev, M. A. Studying the decomposition of monoethanolamine in water using efficient oxidation processes. *Therm. Eng.* **2011**, *58*, 535−539.
(33) Tessier, A.; Forst, W. Mechanism of hydrogen peroxide pyrolysis. *Can. J. Chem.* **1974**, *52*, 794−797.
(34) Hiroki, A.; Laverne, J. A. Decomposition of hydrogen peroxide at water−ceramic oxide interfaces. *J. Phys. Chem. B* **2005**, *109*, 3364−3370.
(35) Park, J. H.; Yoo, Y. B.; Lee, K. H.; Jang, W. S.; Oh, J. Y.; Chae, S. S.; Baik, H. K. Low-temperature, high-performance solution-processed thin-film transistors with peroxo-zirconium oxide dielectric. *ACS Appl. Mater. Interfaces* **2013**, *5*, 410−417.
(36) Kang, D.; Lim, H.; Kim, C.; Song, I.; Park, J.; Park, Y. Amorphous gallium indium zinc oxide thin film transistors: Sensitive to oxygen molecules. *Appl. Phys. Lett.* **2007**, *90*, 192101.
(37) Park, J.-S.; Jeong, J. K.; Chung, H.-J.; Mo, Y.-G.; Kim, H.-D. Electronic transport properties of amorphous indium−gallium−zinc oxide semiconductor upon exposure to water. *Appl. Phys. Lett.* **2008**, *92*, 072104.
(38) Hwang, Y. H.; Seo, J.-S.; Yun, J. M.; Park, H.; Yang, S.; Park, S.-H. K.; Bae, B.-S. An 'aqueous route' for the fabrication of low-temperature-processable oxide flexible transparent thin-film transistors on plastic substrates. *NPG Asia Mater.* **2013**, *5*, e45.
(39) Meyers, S. T.; Anderson, J. T.; Hung, C. M.; Thompson, J.; Wager, J. F.; Keszler, D. A. Aqueous inorganic inks for low-

temperature fabrication of ZnO TFTs. *J. Am. Chem. Soc.* **2008**, *130*, 17603−17609.
(40) Jiang, K.; Anderson, J. T.; Hoshino, K.; Li, D.; Wager, J. F.; Keszler, D. A. Low-energy path to dense HfO_2 thin films with aqueous precursor. *Chem. Mater.* **2011**, *23*, 945−952.